Failure Tests of Laminated Rubber Bearings

K. ISHIDA, H. SHIOJIRI
Central Research Insitute of Electric Power Industry, Abiko, Japan
M. IIZUKA, K. MIZUKOSHI, K. TAKABAYASHI
Kajima Corporation, Tokyo, Japan

1 INTRODUCTION

Pool type fast breeder reactor (FBR) vessels are subjected to severe thermal loads. The thickness of a vessel wall should be minimized to limit the thermal stress in the wall. This is a disadvantageous restriction on the aseismic design of vessel walls. Making use of a base isolation system is one of the most effective solutions to this problem. Of all the devices required for base isolation systems, laminated rubber bearings play the most essential role. However, there are very few past researches on large-deformation behavior and failure of rubber bearings [1,2]. Because of the lack of full information on ultimate characteristics, it has been difficult to determine quantitatively the aseismic safety margin of base-isolated structures. This paper discusses the ultimate characteristics of laminated rubber bearings on the basis of failure tests conducted by the authors.

The same types of rubber bearing as used here were also employed in the shaking table tests of the FBR plant model [3].

2 TEST SPECIMEN

Three types of rubber bearing – natural rubber bearing (NRB), lead-rubber bearing (LRB), and high-damping rubber bearing (HRB) – were designed specifically for a base isolation system of an FBR plant, assuming a dead load of 500tf for each bearing [4,5]. These full-sized bearings were reduced to 1/15 scale models on the basis of the

Table 1 Similarity law

	Prototype	Model
Lenght	1	1/15
Force	1	$1/15^2$
Stress	1	1
Strain	1	1

Table 2 Specimen list

	NRB LRB	HRB
Design axial stress*1 σ_D (kgf/cm²)	25	31
Rubber layer (mm)×(sheets)	0.6×25	1.38×14
Shape factor S_1*2	40	17
Aspect Ratio S_2*3	7	5

*1 : axial stress corresponding to the design dead load
*2 : one loaded area/force-free area
*3 : diameter/total rubber thickness

Table 3 Mechanical properties of rubber

	NRB LRB	HRB
Hardness(IRHD)	40±5	60±5
Tensile stress at 25% elongation (kgf/cm²)	3.4±1	12.0±2
Tensile strength (kgf/cm²)	>200	>100
Elongation at break (%)	>500	>650

similarity law shown in Table 1. The detail of the specimens are shown in Table 2 and Fig. 1. The mechanical properties of the rubber used are listed in Table 3. In the case of LRB, the similarity conditions are perfectly satisfied with respect not only to mechanical properties but also to geometrical details. Therefore, the design axial stress, the shape factor, and the aspect ratio are exactly the same as those of the full-sized bearing. NRB is the same in details as LRB except for the lead plug. In the case of HRB, the geometrical similarity conditions are not satisfied because in its design more stress was placed upon the similarity to LRB's mechanical properties.

3 LOADING SCHEME

The following definitions are introduced.

Axial strain $\varepsilon = \delta_V / h$
Axial stress $\sigma = P / A$
Shear strain $\gamma = \delta_H / h$
Shear stress $\tau = Q / A$

where δ_V is the axial displacement, δ_H is the lateral displacement, P is the axial force, Q is the shear force, h is the total rubber thickness, and A is the cross sectional area (excluding the rubber cover and a lead plug).

The loading scheme shown in Table 4 was prepared to investigate the large-deformation hysteretic behavior under various combinations of shear and axial forces. The loading program consists of tensile tests and shear tests. Most of the specimens were loaded statically and cyclically, while some of the specimens were loaded dynamically and/or monotonically to evaluate the effect of strain rate and cyclic loading. In the case of

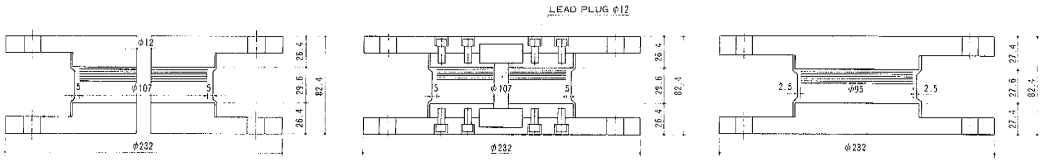

(a) NRB (b) LRB (c) HRB

Fig. 1 Detail of specimens

Table 4 Loading scheme

TENSILE TEST

CASE	OFFSET SHEAR STRAIN γ (%)	STRAIN RATE $\dot{\varepsilon}$ OR FREQUENCY f	LOADING PATTERN
1	0	16%/sec	MONOTONIC
2	0	800%/sec	MONOTONIC
3	0	0.01Hz	CYCLIC
4	200	0.01Hz	CYCLIC
5	300	0.01Hz	CYCLIC
6	400	0.01Hz	CYCLIC
7	465	0.01Hz	CYCLIC

SHEAR TEST

CASE	AXIAL STRESS (+:COMP, −:TENS)	TENSILE STRAIN ε (%)	STRAIN RATE $\dot{\gamma}$ OR FREQUENCY f	LOADING PATTERN
1	σ_0	–	24%/sec	MONOTONIC
2	σ_0	–	1200%/sec	MONOTONIC
3	$\alpha\sigma_0$		0.01Hz	CYCLIC
4	$\alpha\sigma_0$		0.01Hz	CYCLIC
5	0	–	0.01Hz	CYCLIC
6	σ_0	–	0.01Hz	CYCLIC
7	$2\sigma_0$	–	0.01Hz	CYCLIC
8	$3\sigma_0$	–	0.01Hz	CYCLIC
9		50	0.01Hz	CYCLIC
10	–	100	0.01Hz	CYCLIC

$\alpha = -1, -\frac{1}{2}$ (NRB, LRB)
$\alpha = -\frac{1}{2}, -\frac{1}{4}$ (HRB)

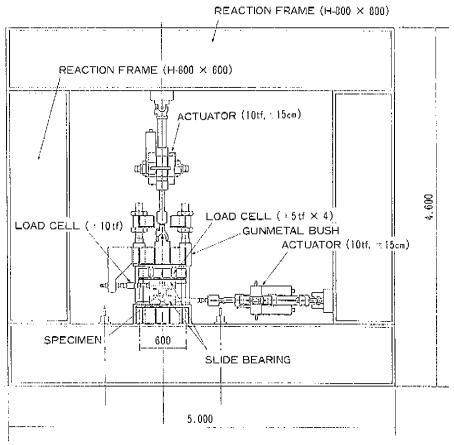

Fig. 2 Testing apparatus

the tensile tests, the offset shear strain, which was kept constant during tensile loading in each test, was selected as a test variable. In the case of the shear tests, the axial stress or the axial strain, which was kept constant during shear loading in each test, was selected as another test variable. A half–cyclic sinusoidal wave of gradually increasing amplitude was used as a tensile strain control signal for the tensile tests. On the other hand, a sinusoidal wave of gradually increasing amplitude was used as a shear strain control signal for the shear tests. In the case of the monotonic loading, specimens were loaded at a constant strain rate. The rapid strain rate was determined so as to be roughly equal to that of the full–sized rubber bearing. In other words, the scale factor for strain rates is the unity in spite of the reduced model.

Fig. 2 shows the testing apparatus. The specimen was mounted on a table which can slide horizontally. The upper flange of the specimen was fixed to a loading block which can move vertically but not rotate. Dynamic actuators were attached to the table and the block. Load cells were arranged so that measurements may not include friction force of the apparatus.

4 TEST RESULTS

4.1 Relationship between stress and strain, and effect of test variables

The tensile stress – strain curves under pure tension shown in Fig. 3 represents the effects of strain rate and cyclic loading. Fig. 4 compares tensile stress – strain envelopes obtained at the different offset shear strain levels. Likewise, the shear stress – strain curves under the design axial stress shown in Fig. 5 represents the effects of strain rate and cyclic loading. Fig. 6 compares shear stress – strain envelopes obtained at the different axial stress or strain levels.

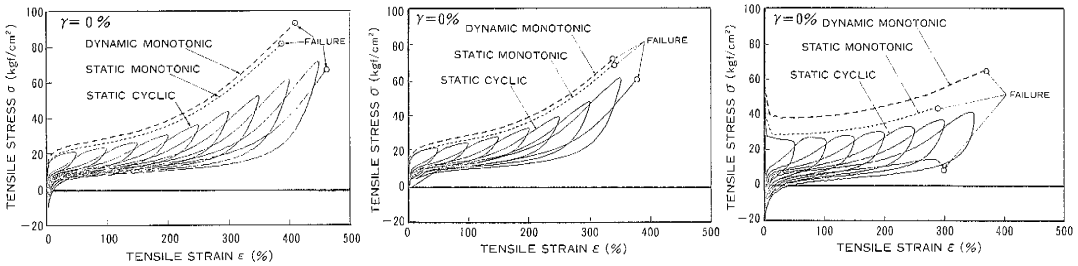

(a) NRB (b) LRB (c) HRB

Fig. 3 Tensile stress – strain curves
(the effect of strain rate and cyclic loading)

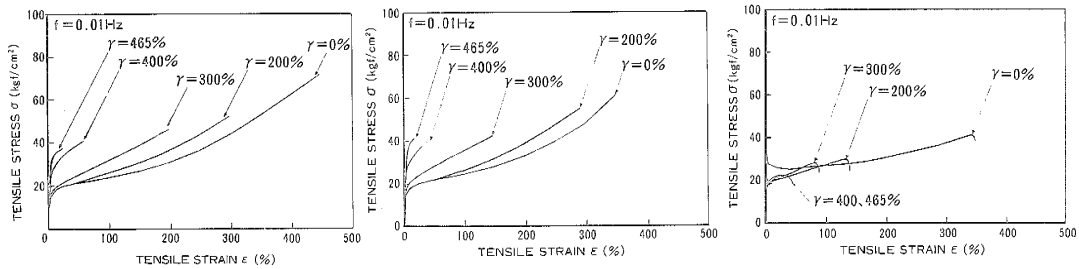

(a) NRB (b) LRB (c) HRB

Fig. 4 Tensile stress –strain envelopes
(the effect of offset shear strain)

Tensile stress – strain relation (See Fig. 3) The tensile stress – strain curves demonstrate that the same tendencies are found in the different types of specimen, that is, high tensile stiffness at extremely low strains, appearance of yield–like phenomenon, low tensile stiffness beyond the " yield" point, and hardening phenomenon at high strains. NRB and LRB show relatively smooth change in stiffness around the yield point and relatively steep hardening slope, while HRB shows a sudden drop in stress around the yield point and a gentle hardening slope.

Effect of offset shear strain on tensile behavior (See Fig. 4) In the case of NRB and LRB, as the magnitude of offset shear strain becomes higher, a yield stress level and post–yield stiffness becomes higher and failure occurs earlier. In the case of HRB, with regard to failure limits, the same tendency is found. However, its yield stress level and post–yield stiffness are not so greatly affected by the offset shear strain level.

Shear stress – strain relation (See Fig. 5) Each type of specimen shows a low shear stiffness within about 200% shear strain and hardening phenomenon beyond this strain level. The hardening slopes of NRB and LRB are rather steep, while that of HRB is relatively gentle.

Effect of axial stress and strain on shear behavior (See Fig. 6) In most cases, shear stress – strain curves of each specimen type are very close to one another in spite of a variety of axial stress and strain conditions. In the case where a high tensile stress or strain is imposed, however, a little higher stiffness and a little earlier failure can be seen compared to the other cases.

Effect of strain rate (See Fig. 3 and Fig. 5) The stress – strain curves and the failure limits of NRB and LRB are almost independent of the strain rate. On the other hand, those of HRB depend greatly on strain rate. In this case, rapid strain rate increases both stress and failure strain level.

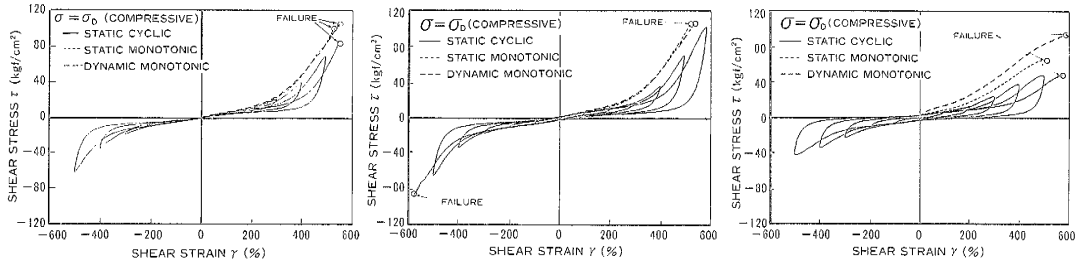

(a) NRB (b) LRB (c) HRB

Fig. 5 Shear stress – strain curves
(the effect of strain rate and cyclic loading)

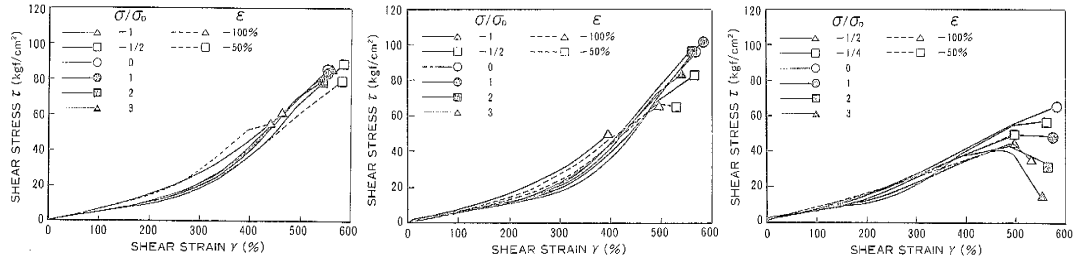

(a) NRB (b) LRB (c) HRB

Fig. 6 Shear stress – strain envelopes
(the effect of axial stress and strain)

Effect of cyclic loading (See Fig. 3 and Fig. 5) Regardless of the specimen type, the cyclic loading decreases stress and increases failure strain level to some extent.

4.2 Failure limit

The maximum stresses and the maximum strains are plotted in an axial stress – shear strain plane, as shown in Fig. 7. All the specimens did not necessarily fail at the maximum points, but the failure points were not so far from the maximum points. The characteristics of these plots can be described as follows : At higt tensile stresses, the maximum tensile stress gradually decreases as the maximum shear strain increases. In the range from small tensile stress to relatively large compressive stress, however, the maximum shear strain level remains almost constant. In this range, the maximum shear strain level ranges from 500% to 600% regardless of specimen type. In most cases, the failure occurred in a rubber layer near the flange, not in an insert plate surface.

4.3 Comparison between NRB and LRB

LRB has the same configuration as NRB except for a lead plug, and so it is interesting to compare them. Comparison in the stress – strain relation and failure limits are shown in Fig. 8. These graphs demonstrate that there is no noticeable difference between NRB and LRB. It should be noted that there is no contribution of a lead plug

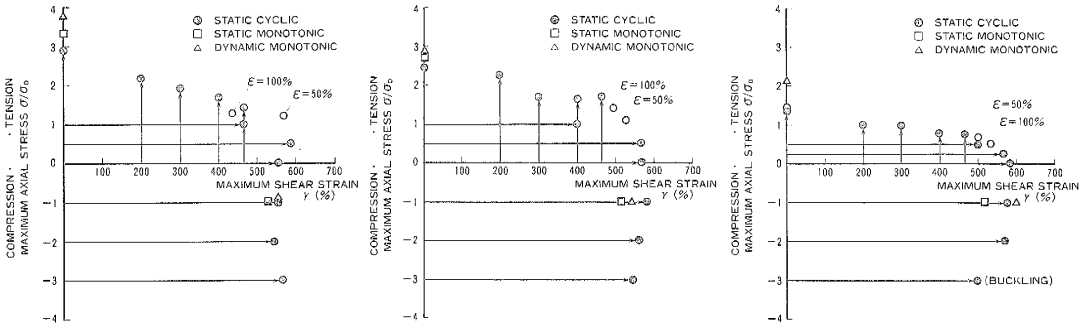

(a) NRB (b) LRB (c) HRB

Fig. 7 Failure limits

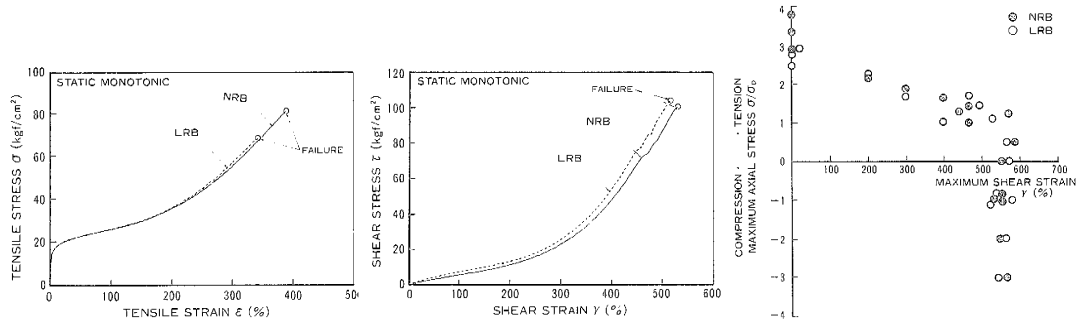

(a) tensile stress – strain curves (b) shear stress – strain curves (c) failure limits

Fig. 8 Comparison between NRB and LRB

to tensile behavior and only slight contribution to large – deformation shear behavior. Furthermore, a lead plug has no bad influence on failure.

5 CONCLUSIONS

Three different types of rubber bearing – natural rubber bearing (NRB), lead–rubber bearing (LRB), and high–damping rubber bearing (HRB) – were tested up to failure under various combinations of axial and shear forces. The test results are summarized as follows :

1) Offset shear strain greatly affects tensile behavior and failure.
2) Axial stress or strain does not so greatly affect shear behavior and failure.
3) The characteristics of NRB and LRB are almost independent of strain rate, but those of HRB depend greatly on it.
4) Cyclic loading affects large–deformation behavior and failure to some extent.
5) Failure limits which include the interaction between axial stress and shear strain were quantitatively evaluated.
6) A lead plug of LRB has no bad influence on failure.

These will be very useful for developing an ultimate response prediction technique, which is necessary to establish rational design philosophy of base isolation systems for FBR plants.

ACKNOWLEDGEMENTS

This research is a part of a research project " Demonstration Test of Seismic Isolation System for Fast Breeder Reactor" sponsored by the Ministry of International Trade and Industry.

REFFERENCES

1. Suzuki,S., Fujita,T. and Shimazaki,M. (1990). High Damping Rubber Bearings for Seismic Isolation of Building (2nd Report, Breaking Tests)(in Japanese) Trans. of the Japan Society of Mechanical Engineers, Vol.56–523C, pp667–672

2. Iizuka,M., Mizukoshi,K., Takabayashi,K. and Ishida,K. (1990). Experimental Evaluation on Ultimate Behavior of Laminated Rubber Bearings. International Fast Reactor Safety Meeting, Vol.3, pp423–429

3. Matsuda,A. et al. (1991). Shaking Table Test on Base Isolated FBR Plant Model. SMIRT11

4. Mazda,A. et al. (1989). Test on Large–Scale Seismic Isolation Elements. SMiRT10, Vol.K2, pp679–684

5. Mazda,A. et al. (1991). Test on Large–Scale Seismic Isolation Elements. SMiRT11